Molecular Cell Biology

Cancer Research

The MDA-9/Syntenin/IGF1R/STAT3 Axis Directs Prostate Cancer Invasion

Swadesh K. Das[1,2,3], Anjan K. Pradhan[1], Praveen Bhoopathi[1], Sarmistha Talukdar[1], Xue-Ning Shen[1], Devanand Sarkar[1,2,3], Luni Emdad[1,2,3], and Paul B. Fisher[1,2,3]

Abstract

Although prostate cancer is clinically manageable during several stages of progression, survival is severely compromised once cells invade and metastasize to distant organs. Comprehending the pathobiology of invasion is required for developing efficacious targeted therapies against metastasis. Based on bioinformatics data, we predicted an association of melanoma differentiation-associated gene-9 [syntenin, or syndecan binding protein (SDCBP)] in prostate cancer progression. Using tissue samples from various Gleason stage prostate cancer patients with adjacent normal tissue, a series of normal prostate and prostate cancer cell lines (with differing tumorigenic/metastatic properties), *mda-9/syntenin*-manipulated variants (including loss-of-function and gain-of-function cell lines), and CRISPR/Cas9 stable MDA-9/Syntenin knockout cells, we now confirm the relevance of and dependence on MDA-9/syntenin in prostate cancer invasion. MDA-9/Syntenin physically interacted with insulin-like growth factor-1 receptor following treatment with insulin-like growth factor binding protein-2 (IGFBP2), regulating downstream signaling processes that enabled STAT3 phosphorylation. This activation enhanced expression of MMP2 and MMP9, two established enzymes that positively regulate invasion. In addition, MDA-9/syntenin-mediated upregulation of proangiogenic factors including IGFBP2, IL6, IL8, and VEGFA also facilitated migration of prostate cancer cells. Collectively, our results draw attention to MDA-9/Syntenin as a positive regulator of prostate cancer metastasis, and the potential application of targeting this molecule to inhibit invasion and metastasis in prostate cancer and potentially other cancers.

Significance: This study provides new mechanistic insight into the proinvasive role of MDA-9/Syntenin in prostate cancer and has potential for therapeutic application to prevent prostate cancer metastasis. *Cancer Res; 78(11); 2852–63. ©2018 AACR.*

Introduction

As for most solid malignancies, mortality from prostate cancer, the most commonly diagnosed noncutaneous cancer, results from widespread metastases (1). In this context, even treatment of localized prostate cancer is fraught with significant morbidity; however, once metastasis occurs, there are few available treatment options for patients that have failed to respond to androgen deprivation therapies. Patients diagnosed in this advanced stage usually die within 12 to 18 months (1), emphasizing the need for better definition of the signaling cascades that regulate metastasis, which embodies three main processes: invasion, intravasation, and extravasation. Invasion initiates with loss of cell–cell adherence of metastatic competent cells, which become motile and breakdown the extracellular matrix, allowing them to migrate and enter the circulation (2). Multiple intrinsic transcriptional and epigenetic molecular programs regulate epithelial-to-mesenchymal transition (EMT). This process results in loss of intracellular adhesion and epithelial polarization, cytoskeleton rearrangement facilitating mobility, and release of extracellular proteases including matrix metalloproteinases (MMP) that degrade the extracellular matrix promoting tumor spread. Secretion of active MMPs releases matrix-bound growth factors and cytokines further enabling invasion (3).

Defining genes that control invasion has potential to identify new target(s) for intervening in metastasis, which would have profound therapeutic implications. To achieve this objective, we employed subtraction hybridization (4). *Melanoma differentiation-associated gene-9* (*mda-9*), also known as *syntenin* (*mda-9/syntenin*), was initially identified by subtraction hybridization as a novel gene displaying biphasic expression during terminal differentiation of human melanoma cells (5, 6). MDA-9/Syntenin, a PDZ-domain protein, overexpressed in many types of human cancers, based on bioinformatics analyses (http://cancergenome.nih.gov/), may function in tumor progression (7–9). Although both bioinformatics analyses and our observations (published and unpublished) indicate a positive correlation of *mda-9/syntenin* expression with aggressive phenotypes in multiple cancers, the precise roles of *mda-9/syntenin* in many of these neoplasms have not been ascertained. Suppression subtractive hybridization between a poorly invasive/nonmetastatic and an invasive/metastatic breast cancer cell line identified *mda-9/syntenin* overexpression in metastatic cells (10). Overexpression of *mda-9/syntenin* is also evident in metastatic melanoma (11), breast (10), gastric (10), and bladder (12) cancer cells in comparison with their

[1]Department of Human and Molecular Genetics, Virginia Commonwealth University, School of Medicine, Richmond, Virginia. [2]VCU Institute of Molecular Medicine, Virginia Commonwealth University, School of Medicine, Richmond, Virginia. [3]VCU Massey Cancer Center, Virginia Commonwealth University, School of Medicine, Richmond, Virginia.

Note: Supplementary data for this article are available at Cancer Research Online (http://cancerres.aacrjournals.org/).

Corresponding Authors: Paul B. Fisher, Virginia Commonwealth University, School of Medicine, 1101 East Marshall Street, Sanger Hall Building, Room 11-015, Richmond, VA 23298. Phone: 804-628-3506; Fax: 804-827-1124; E-mail: paul.fisher@vcuhealth.org; and Swadesh K. Das, E-mail: swadesh.das@vcuhealth.org

doi: 10.1158/0008-5472.CAN-17-2992

primary or poorly metastatic counterparts. Recently, we confirmed a role of this protein in glioma invasion (13). Notably, forced expression of *mda-9/syntenin* increased migration of nonmetastatic cancer cells, which correlated with a more polarized distribution of F-actin and increased pseudopodia formation (11, 14). In addition, immunohistochemical analyses revealed a statistically significant continued increase in MDA-9/Syntenin expression from acquired melanocytic nevi to primary melanoma without or with progression to metastatic melanoma. These accumulated data strongly support the hypothesis that *mda-9/syntenin* functions as a positive regulator of melanoma metastasis (11, 15–17) as well as aggressiveness in breast and gastric cancers (10), and might contribute to invasion of multiple additional cancers.

The insulin-like growth factor (IGF) signaling axis plays a pivotal role in prostate cancer progression, confirmed both in preclinical and clinical studies (18). This signaling axis consists of extracellular ligands (IGF1 and IGF2 with their binding partners, e.g., IGFBP1 to -6) and receptors (IGF1R and IGF2R for IGF1 and IGF2, respectively). In 1998, Chan and colleagues first reported a positive correlation between IGF1 levels and prostate cancer risk (19), which was validated further in transgenic animals overexpressing IGF1 in prostate epithelium that led to spontaneous neoplasia in the mouse prostate (20, 21). Upon stimulation by specific ligands, IGF1R is activated through autophosphorylation, resulting in phosphorylation of its downstream targets insulin receptor substrate-1 (IRS1) and Shc adaptor proteins, which play decisive roles in cellular proliferation/differentiation/cellular homeostasis through PI3K/AKT or Ras/Raf/Mek pathways (22). In addition, activation of IGF1R also associates with cellular invasiveness and metastatic phenotypes through activation of IRS1 that directly influences the β-catenin pathway (23), or by regulating secretion of MMPs (24). As a receptor kinase, IGF1R influences other growth factors or receptors such as VEGF and EGFR (reviewed by Tao and colleagues; ref. 25) and regulates angiogenesis and proliferation. Accordingly, IGF1R activation or its signaling cascade in prostate cancer is fundamental, emphasizing clinical relevance and rationalizing the development of targeted therapeutics as reflected by the accelerated number of ongoing clinical trials employing inhibitors of the IGF1R axis (reviewed by Heidegger and colleagues; ref. 22).

The present study explores the relevance of MDA-9/Syntenin expression in prostate cancer pathogenesis. We decipher a novel mechanistic signaling pathway for MDA-9/Syntenin in regulating prostate cancer invasion. IGF1R, through a physical interaction with MDA-9/Syntenin, is central in this cascade. Overall, our findings show that MDA-9/Syntenin represents a novel molecular target for inhibiting invasion and metastasis, an ultimate cause of prostate cancer–associated death.

Materials and Methods

Human cell lines

In the present study, the following cell lines were used: P69, RWPE-1, DU-145, PC-3, M12, M2182, ARCaP, ARCaP-E, and ARCaP-M (26). P69 (SV40 T antigen immortal normal human prostate epithelial cells), M2182 (progressed P69 cells displaying a tumorigenic phenotype), and M12 (progressed P69 cells displaying a tumorigenic and metastatic phenotype) were provided by Dr. Joy Ware, VCU School of Medicine, Richmond, VA. P69, M2182, and M12 provide a representative panel of human prostate cells (from normal immortal, tumorigenic, metastatic) and are described and cultured as indicated in our previous publication (26). Other cells, except ARCaP with its epithelial and metastatic variants, ARCaP-E and ARCaP-M, respectively, were obtained from the ATCC and maintained in culture as per the ATCC recommendations. ARCaP, ARCaP-E, and ARCaP-M cells were from Novicure Biotechnology and maintained in media recommended by the provider. HPV-immortal human prostate epithelial cells, RWPE-1, were from the ATCC. All cell lines were routinely checked for mycoplasma contamination using commercial kits. The majority of experiments used RWPE-1, DU-145, and ARCaP-M cells. All of these cell lines were purchased recently (within the last 3 years) and were strictly maintained as recommended by the manufacturer.

Reagents and antibodies

Specific antibodies [MDA-9/Syntenin, Phospho-IGF1R (Tyr-1135), IGF1R, Phospho-Src (Tyr-416), Src, Phospho-FAK (Tyr-397), FAK, Phospho-STAT3 (Tyr-705), MMP2, MMP9, IGFBP2, STAT3, Syntenin-2, β-actin and EF-1α] and reagents [IGFBP2 and ELISA kits (IGFBP2)] used in the present study are described in Supplementary Materials and Methods.

Tissue microarray

Two different prostate cancer tissue microarrays (TMA), purchased from Novus Biologicals and USBiomax, were stained with MDA-9/Syntenin or IGFBP2 antibody from Sigma-Aldrich. All clinical samples were received from a commercial source without any personal identifications, with the exception of sex (all are male), age, and cancer stage. Images were captured by Vectra Polaris Quantitative Pathology Imaging System in VCU Cancer Mouse Models Developing Shared Resource Core. Staining intensity was quantified with inbuilt software supplied by PerkinElmer, Inc.

Real-time PCR

For qPCR, total RNA was extracted using miRNeasy kits (Qiagen), and cDNA was prepared as described (15). Quantitative qPCR was performed using an ABI ViiA7 fast real-time PCR system and Taqman gene expression assays according to the manufacturer's protocol (Applied Biosystems).

Constructs and stable cell clones

Vectors and stable cell clones used in this study, including *mda-9* and sh*mda-9* (15), and pRc.CMV.Stat3Y705F vectors and Pool 1 and Pool 2 *mda-9/syntenin* knockout, and *sgRNA control* clones are described in Supplementary Materials and Methods.

In vivo experiments

All *in vivo* experiments were performed using Institutional Animal Care and Use Committee–approved protocols. Metastasis assays using tail vein injection were performed by injecting 1×10^6 ARCaP-M-Luc cells, either infected with Ad.5/3-sh*con* or Ad.5/3-sh*mda-9*, and animals were monitored for lung fluorescence by bioluminescence at 48 days, and survival was monitored over 90 days. Details can be found in Supplementary Materials and Methods.

Coimmunoprecipitation

Coimmunoprecipitation was performed as described previously (15, 17) using a kit from Pierce (Pierce Biotechnology).

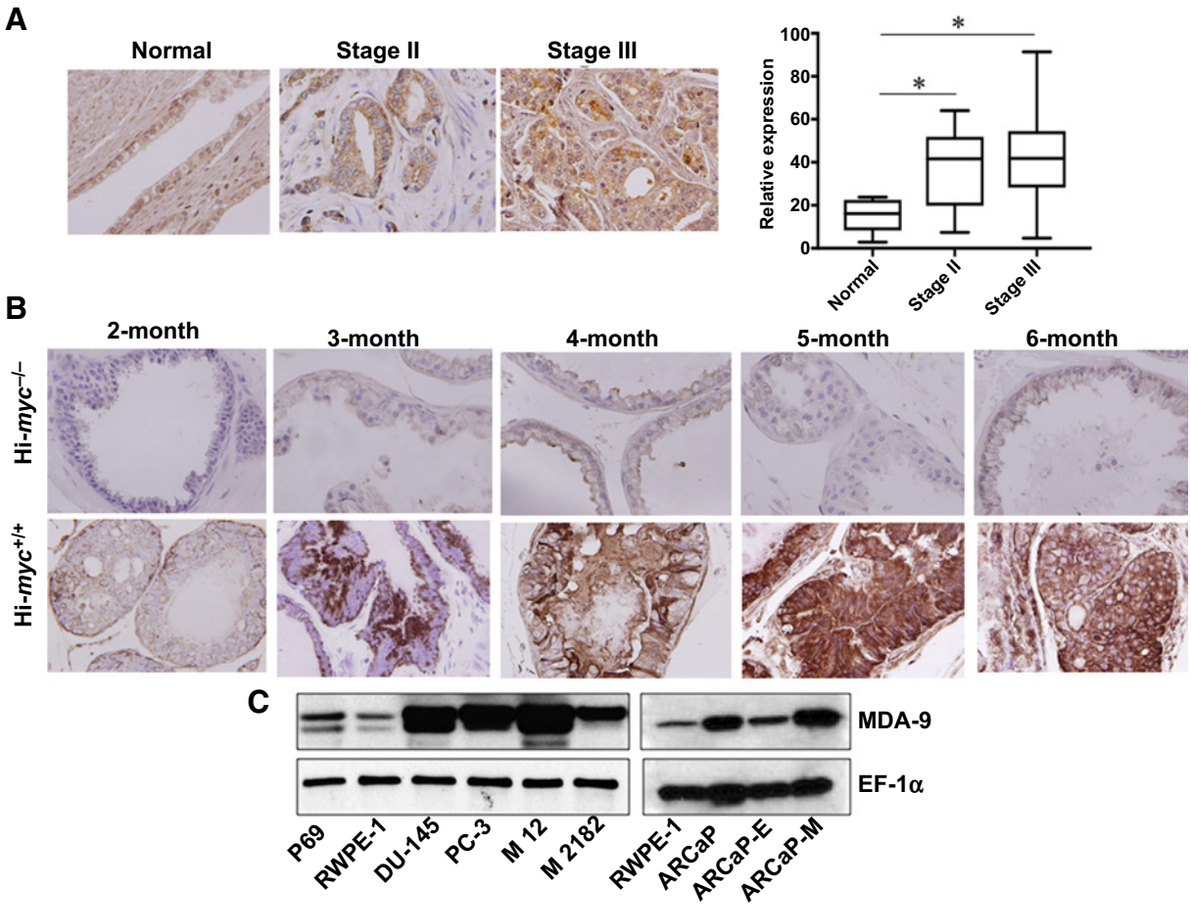

Figure 1.

MDA-9/Syntenin is upregulated in advanced prostate cancer. **A,** Representative photomicrographs of MDA-9/Syntenin expression in various stages of prostate adenocarcinoma. Staining intensity was measured using imaging software, and the average value with SD for stage II and III disease is presented. **B,** Prostates from Hi-*Myc*–positive or –negative male mice at different ages ($n = 3$) were collected, paraffin embedded, and sectioned. Representative photomicrographs of MDA-9/Syntenin-immunostained slides. **C,** Expression of MDA-9/Syntenin in P69, RWPE-1, and different human prostate cancer cells.

Invasion assays

Boyden chamber assays tested the invasive properties of cancer cells (15, 17). Briefly, cells were infected with control shRNA or *mda-9/syntenin* shRNA expressing Ad.5/3 and plated on the Matrigel-coated upper chamber. After 18 hours, invasive cells in the lower chamber were photographed and analyzed. All data presented mean ± SD.

Statistical analysis

All data represent mean ± SD from three independent experiments. Statistical analysis was performed using either the Student *t* test (Microsoft Excel) or Pearson correlation (GraphPad prism software). $P < 0.05$ was considered significant.

Results

MDA-9/Syntenin expression is elevated in prostate cancer

Computational analysis identified *mda-9/syntenin* mRNA overexpression in prostate cancer compared with normal prostate (8). Immunohistochemistry of MDA-9/Syntenin protein expression in two TMA slides containing 8 adjacent tumor tissue sections and 64 human prostate tumor samples (from individual patients) at different disease stage [stage II ($n = 17$) and stage III ($n = 47$)] supported the genomic profiling data (Fig. 1A). MDA-9/Syntenin expression was significantly upregulated in stages II and III compared with adjacent normal tissue. Due to the low number of cases, samples from "stage I ($n = 3$)," "metastatic stage ($n = 2$)," "hyperplasia ($n = 3$)," "small acinar carcinoma ($n = 1$)," and "carcinoid ($n = 1$)" were not included in the final analysis. In the two cases from metastatic stage, higher expression of MDA-9/Syntenin was observed; however, the staining scores were not significantly different from stage III adenocarcinoma. Next, prostate tumor sections from a cohort of Hi-*myc* mice, a well-studied spontaneous prostate cancer model that develops PIN by 13 weeks and invasive adenocarcinoma by 26 weeks of age, were analyzed for MDA-9/Syntenin expression (27). In 2-month-old and older Hi-*myc* mice, MDA-9/Syntenin expression was elevated in prostate adenocarcinomas (Fig. 1B).

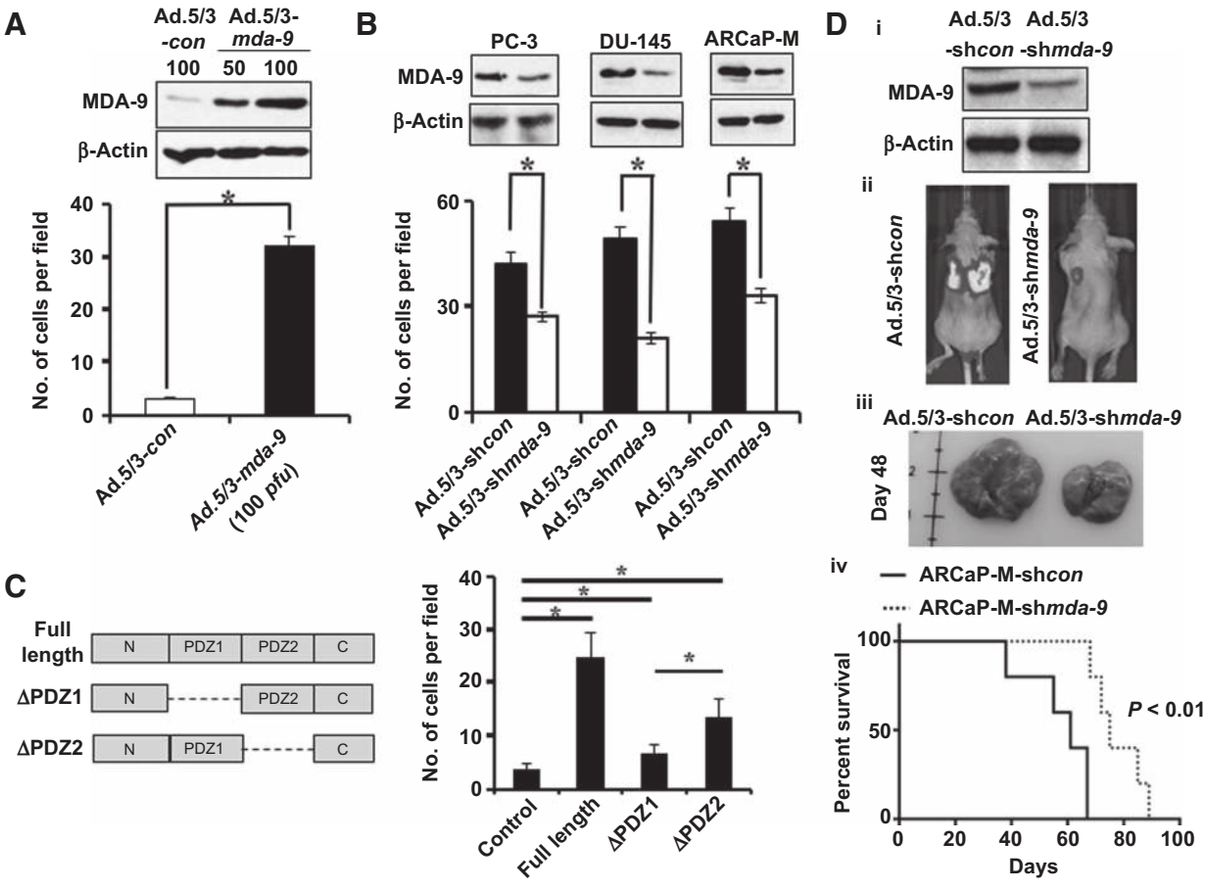

Figure 2.

MDA-9/Syntenin regulates prostate cancer progression. **A,** RWPE-1 cells infected with various adenoviruses at the indicated multiplicity of infection. After 48 hours, infected cells were subjected to Matrigel invasion assays as described in Materials and Methods. Expression of MDA-9/Syntenin was confirmed by Western blotting. **B,** MDA-9/Syntenin levels and invasiveness of different prostate cancer cells after infection with Ad.5/3-sh*con* or Ad.5/3-sh*mda-9*. **C,** Left, schematic diagram of mutant *mda-9/syntenin* constructs, ΔPDZ1 and ΔPDZ2. Right, RWPE-1 cells transfected with full length and mutants of *mda-9/syntenin*, and 48 hours after transfection, invasion was evaluated. Number of invaded cells presented as a bar graph. Average with SD from three independent experiments. *, statistical significance ($P < 0.05$) between indicated groups. **D, i,** Downregulation of MDA-9/Syntenin was confirmed in Ad. sh*mda-9*–infected cells. Luciferase-expressing ARCaP-M cells carrying sh*con* or sh*mda-9* were inoculated i.v. into athymic nude mice by tail vein. Representative photographs of BLI (**ii**) and gross morphology of lungs (**iii**) 48 days after inoculation. **iv,** Kaplan–Meier survival graph using Graph Pad software.

MDA-9/Syntenin was elevated (Fig. 1C; Supplementary Fig. S1) in different human prostate cancer cell lines in comparison with RWPE-1, a normal immortalized prostate epithelial cell line. Expression was significantly upregulated in M12, a metastatic variant of P69 (immortalized prostate epithelial cells), suggesting an association of MDA-9/Syntenin with metastasis, which was supported further by *in vitro* invasion assays. MDA-9/Syntenin was also overexpressed in M2182 cells, which are tumorigenic but nonmetastatic P69 variant cells, suggesting that in addition to metastasis, MDA-9/Syntenin might also contribute to tumorigenic phenotypes. In addition, higher expression of MDA-9/Syntenin was evident in mesenchymal ARCaP-M (metastatic variant) cells in comparison with epithelial variant ARCaP-E cells (Fig. 1C, right; Supplementary Fig. S1), providing additional confirmation of the potential relevance of MDA-9/Syntenin in prostate cancer progression.

MDA-9/Syntenin expression regulates invasiveness of prostate cancer cells

Invasion is an early event in metastasis (28). A role of MDA-9/Syntenin in invasion has been established in multiple cancer lineages (9). To investigate the potential role of this gene in prostate cancer invasion, we overexpressed *mda-9/syntenin* in normal immortal RWPE-1 cells, using an adenovirus-expressing *mda-9/syntenin* (Ad.5/3-*mda-9*; refs. 15, 17). Adenovirus-expressing empty vector was used as control. Overexpression of *mda-9/syntenin* (Supplementary Fig. S2A) caused a robust upregulation of invasion ability (~6-fold) in these minimally invasive cells (Fig. 2A). In addition, we silenced MDA-9/Syntenin expression in three aggressive human prostate cancer cell lines, PC-3, DU-145, and ARCaP-M, using an *mda-9/syntenin*-targeted shRNA carrying adenovirus (Ad.5/3-sh*mda-9*; refs. 15, 17). A significant reduction (~30% to ~50%) in invasion was observed, which correlated with the downregulation of

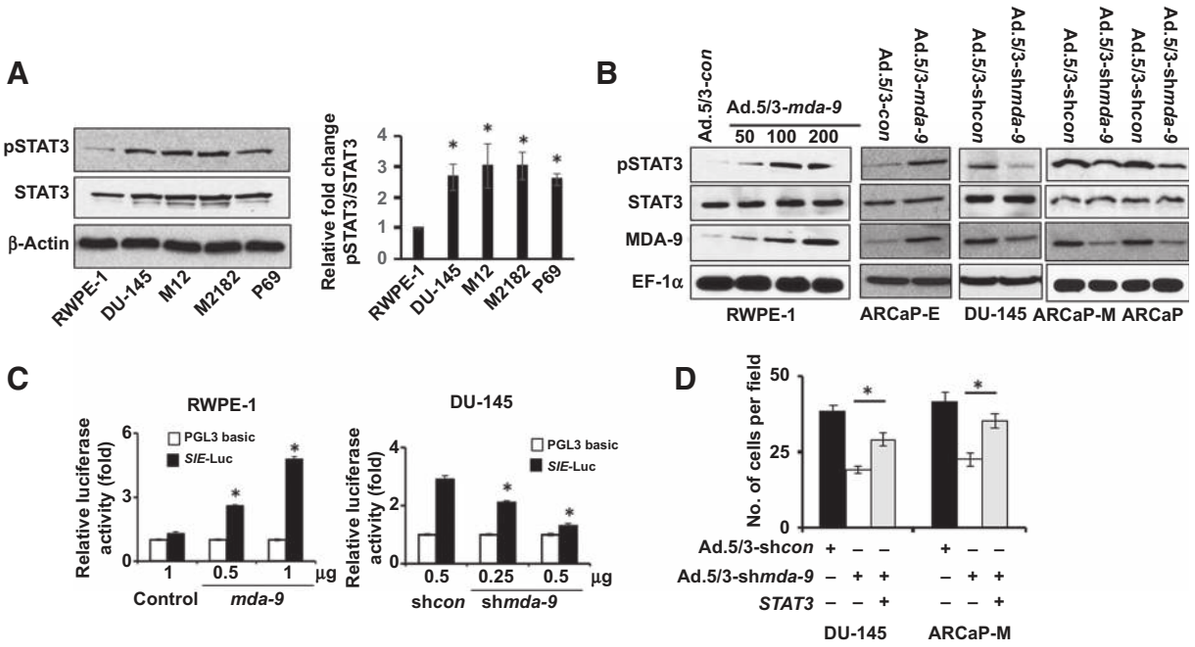

Figure 3.

MDA-9/Syntenin regulates STAT3 activity in prostate cancer cells. **A,** Western blotting analysis of phospho-STAT3 (Tyr705) and total STAT3 (left). Band intensity was quantified, and relative-fold change in different cancer cells vs. RWPE-1 is presented (right). Average with SD from three independent experiments. *, statistical significance ($P < 0.05$) between indicated groups. **B,** Cells were infected with indicated adenoviruses for 48 hours and reseeded on fibronectin-coated plates. Total cell lysates prepared 1 hour after plating and Western blotting using indicated antibodies. **C,** Cells were cotransfected with a reporter gene and empty vector, *mda-9/syntenin,* or *mda-9/syntenin* shRNA, and after 48 hours, luciferase activity was measured. Data presented as fold-change vs. the control group (empty vector). **D,** Cells were cotransfected with different expression plasmids, and 48 hours later, cells were trypsinized and invasion assayed. Cells counted using brightfield microscopy.

MDA-9/Syntenin expression (Fig. 2B; Supplementary Fig. S2B). Both PDZ domains affect MDA-9/Syntenin-mediated invasion, because ectopic expression of mutant constructs (Fig. 2C, left panel, ΔPDZ1 and ΔPDZ2; refs. 16, 29) containing only the PDZ1 (ΔPDZ2) or PDZ2 (ΔPDZ1) domain decreased invasion as compared with full-length *mda-9/syntenin* (WT; Fig. 2C, right). Deletion of the PDZ1 domain had greater impact on invasion than deleting the PDZ2 domain in prostate cancer cells (Student *t* test, $P = 0.0002$). MDA-9/Syntenin expression was manipulated by infecting cells with Ad.5/3-sh*mda-9* and introduced into athymic nude mice intravenously via tail vein injection. Mice were imaged to monitor lung metastasis progression. Tumor burden was reduced in the lungs of animals that received *mda-9/syntenin*-manipulated (suppressed, Fig. 2D, i) ARCaP-M-Luc cells (Fig. 2D, ii). Mice receiving control cells had larger lungs (Fig. 2D, iii) and poorer survival in comparison with the *mda-9/syntenin*-manipulated (suppressed) group (Fig. 2D, iv).

MDA-9/Syntenin regulates prostate cancer invasion through STAT3 activation

Many tumor-derived cell lines as well as human tumors, including prostate cancer, express a constitutively active STAT3 protein (30–32). Consistent with previous observations, STAT3 activity (measured by phosphorylated (Tyr705) STAT3) was significantly higher in three aggressive prostate cancer cells and showed a positive correlation with MDA-9/Syntenin levels (Fig. 3A vs. Fig. 1C for MDA-9/Syntenin). Next, we assessed the expression of phospho-STAT3 by Western blotting in *mda-9/syntenin*-overexpressing RWPE-1 cells or in different prostate cancer cells where *mda-9/syntenin* was silenced. As seen in Fig. 3B, forced expression of *mda-9/syntenin* upregulated STAT3 activation in RWPE-1 and ARCaP-E cells (Supplementary Fig. S3). Conversely, downregulation of *mda-9/syntenin* in different prostate cancer cells (DU-145, ARCaP, and ARCaP-M) negatively regulated STAT3 activation, supporting a correlation between MDA-9/Syntenin expression and STAT3 activity (Supplementary Fig. S3). To provide additional confirmatory evidence, an additional experiment was conducted using STAT3 reporter constructs from SA Bioscience, which encode a firefly luciferase reporter gene under the control of a minimal CMV promoter and tandem repeats of the SIE transcriptional response element. These constructs can monitor both increases and decreases in the transcriptional activity of STAT3-containing dimers, and hence the activity of the STAT3 signaling pathway. Evidence for *mda-9/syntenin*-mediated STAT3 activation was verified by cotransfection of a STAT3 reporter with *mda-9/syntenin* or sh*mda-9* in RWPE-1 and DU-145 cells, respectively (Fig. 3C). Finally, the anti-invasive activity of *mda-9/syntenin* silencing was rescued by overexpressing a constitutively active STAT3 in transiently *mda-9/syntenin* knockdown prostate cancer cells (Fig. 3D). Blocking secretion, using Brefeldin A, significantly reduced STAT3 activity in DU-145 and ARCaP-M cells, indicating a role of secretion in activation (Fig. 4A). To further characterize the secretory molecules involved in MDA-9/Syntenin-mediated STAT3 regulation, we evaluated the role

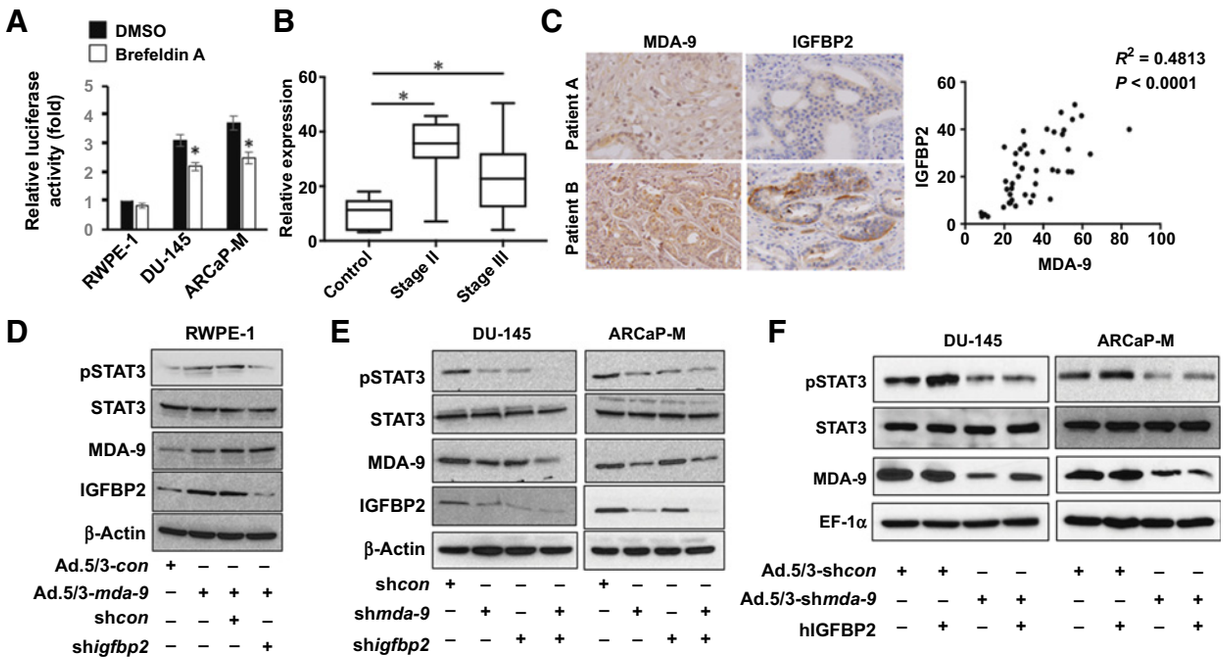

Figure 4.

MDA-9/Syntenin plays a decisive role in IGFBP2–induced STAT3 activation. **A,** Cells transfected with a STAT3 reporter gene and after 36 hours were treated with Brefeldin A (5 μg/mL) for 30 minutes. Media were removed, and cells were cultured for an additional 3 hours in serum-free media and luciferase activity measured. **B,** Immunostaining for IGFBP2 was performed in tissue microarray, and staining intensity was quantified with Polaris Image Analysis software. The average value with SD from different stages is plotted. *, statistical significance between groups. **C,** The expression of MDA-9/Syntenin and IGFBP2 correlates in sections from the same patient (top, patient A, low expression; bottom, patient B, high expression). Pearson correlation determined using 46 samples and presented with R^2 and P value. **D,** RWPE-1 cells expressing MDA-9/Syntenin were cultured in presence of control shRNA or *igfbp2* shRNA for 48 hours. Cells were trypsinized and reseeded onto fibronectin-coated plates. Samples were collected after 1 hour, and Western blotting was performed. **E,** Endogenous MDA-9/Syntenin and IGFBP2 expression in prostate cancer cells treated with sh*mda-9* and sh*igfbp2* either alone or in combination. Cells were reseeded on fibronectin-coated plates for 1 hour. Western blotting with indicated antibodies. **F,** Prostate cancer cells infected with Ad.5/3-sh*con* or Ad.5/3-sh*mda-9* (100 pfu/cell) for 48 hours. Cells reseeded on fibronectin-coated plates and treated with recombinant hIGFBP2 (100 ng/mL) for 1 hour. Western blotting for indicated proteins.

of IGFBP2, a downstream secretory target of MDA-9/Syntenin (15), which was expressed at elevated levels in aggressive prostate cancer cells (33, 34). A TMA slide (Novus Biologicals) was immunostained for IGFBP2 and compared with MDA-9/Syntenin-stained sections. In 46 samples, including both normal ($n = 8$) and adenocarcinomas (8 and 30 cases from stages II and III, respectively), both stage II and III cases showed significantly higher staining intensity compared with adjacent normal tissue (Fig. 4B). The values for MDA-9/Syntenin and IGFBP2 from individual cases were analyzed for Pearson correlation using statistical software (Prism). A positive correlation ($r^2 = 0.4813$, $P < 0.0001$) between these two proteins was observed when comparing the 46 samples (Fig. 4C) or only stage II ($n = 8$, $r^2 = 0.8451$, $P < 0.0083$) and stage III ($n = 30$, $r^2 = 0.5965$, $P < 0.0005$) samples. In addition, when comparing ARCaP series for both *mda-9/syntenin* and *IGFBP2* mRNA expression, maximum fold changes (relative to RWPE-1) for both genes were evident in ARCaP, followed by ARCaP-M and ARCaP-E (Supplementary Fig. S4A). Similar patterns were also apparent in DU-145 and PC-3ML cells (metastatic prostate cancer cells isolated from a bone metastatic lesion; Supplementary Fig. S4A). Finally, using a loss-of-function experiment, we confirmed that *mda-9/syntenin* expression directly regulates *igfbp2* at both mRNA and protein levels (Supplementary Fig. S4B and S4C). In contrast, manipulation of MDA-9/syntenin did not alter the expression of Syntenin-2 (Supplementary Fig. S4C and S4D). Downregulation of secretory IGFBP2 was evident by ELISA in the media collected from *mda-9/syntenin*-manipulated cell lines (Supplementary Fig. S4E). Cotransfection studies with various combinations of genetic manipulation defined the effects of IGFBP2 on STAT3 activation and the potential role of MDA-9/Syntenin in this pathway. RWPE-1 cells, which have very low levels of MDA-9/Syntenin expression, displayed higher STAT3 activity following elevated *mda-9/syntenin* expression. This activity was significantly suppressed in the presence of sh*igfbp2*, indicating the importance of IGFBP2 (Fig. 4D; Supplementary Fig. S5A) in MDA-9/Syntenin-mediated STAT3 activation. Similarly, transiently silencing *mda-9/syntenin* affected STAT3 activation in DU-145 and ARCaP-M cells, and the effect was more robust when both genes (*mda-9/syntenin* and *igfbp2*) were knocked down (Fig. 4E; Supplementary Fig. S5B). Loss-of-function studies in ARCaP-M and DU-145 cells confirmed that exogenous hIGFBP2 (recombinant protein)–mediated STAT3 activation depended on endogenous MDA-9/Syntenin expression levels (the effects of hIGFBP2 were not evident in *mda-9/syntenin*-knockdown cells, Fig. 4F; Supplementary Fig. S5C).

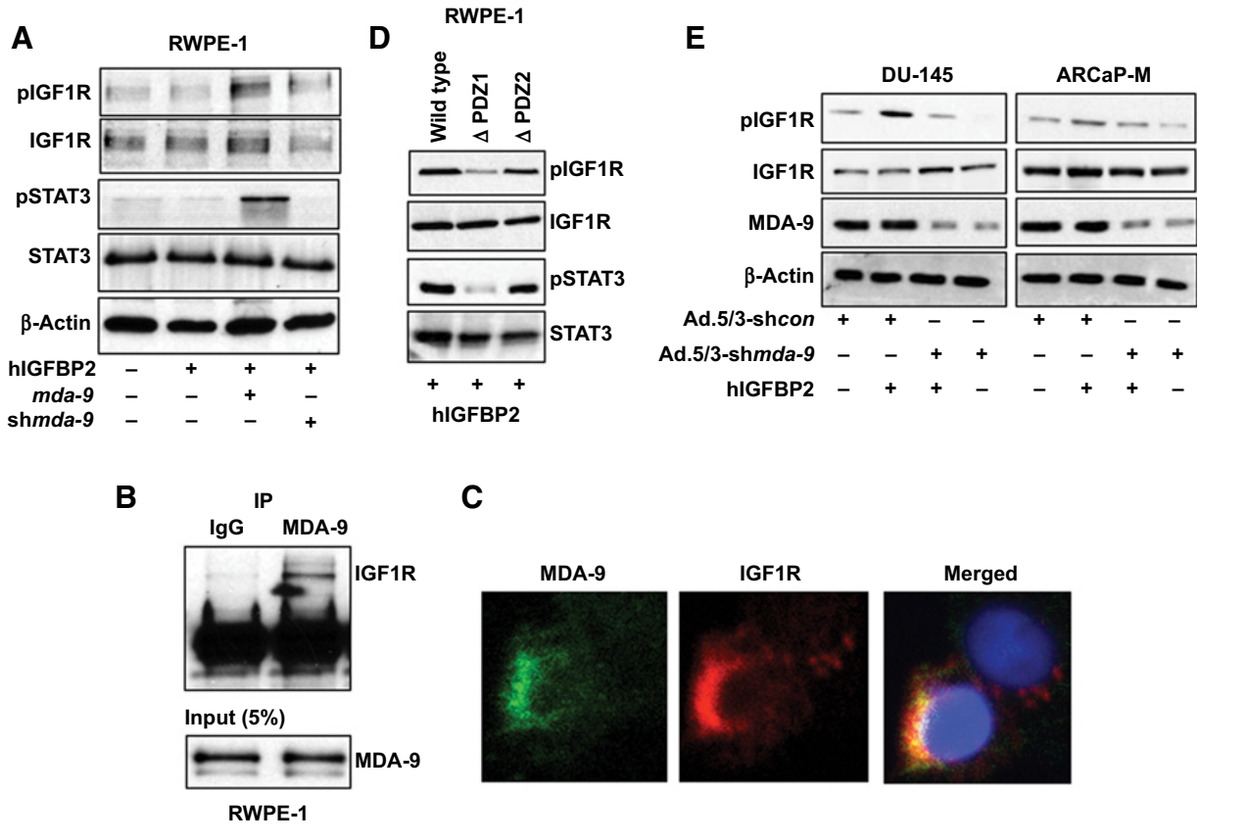

Figure 5.

IGF1R and MDA-9/Syntenin physically interact and regulate STAT3 activity. **A,** RWPE-1 cells treated with hIGFBP2 under different conditions and phospho-IGF1R expression determined by Western blotting. **B,** 200 μg of total protein from ARCaP-M cells incubated with MDA-9/Syntenin overnight for immunoprecipitation, and Western blotting was performed with anti–IGF1R antibody. **C,** Immunofluorescence assay to determine colocalization of proteins. Confocal microscopy images of MDA-9/Syntenin and IGF1R as "separate" or "merged" images. **D,** RWPE-1 cells transfected with wild-type or mutant *mda-9* vectors. Forty-eight hours later, cells were replated on fibronectin-coated plates for 30 minutes and cell lysates were analyzed using the indicated antibodies. **E,** Prostate cancer cell lines were infected with Ad.5/3-sh*con* or Ad.5/3-sh*mda-9* for 48 hours. Cells were reseeded on fibronectin-coated plates and were treated with recombinant hIGFBP2 (100 ng/mL) for 1 hour. Western blotting analysis was done to determine autophosphorylation.

MDA-9/Syntenin physically interacts with IGF1R and activates STAT3

IGF1R is a tyrosine kinase that phosphorylates STAT3 (35). IGF1R, which belongs to the IGF receptor family, is a transmembrane receptor tyrosine kinase. In response to IGF1 ligand binding, IGF1R is activated via autophosphorylation (Tyr 980), leading to activation of various signaling cascades including STAT3. Because IGF1R can also potently activate the STAT3 pathway, one could envision a model in which IGFBP2 (through binding with IGF1) might activate STAT3 in an IGF1R–dependent manner. To explore this possibility, we treated RWPE-1 with recombinant IGFBP2 (hIGFBP2) in the absence of serum, and Western blotting was performed to determine autophosphorylation, representing the activation state of IGF1R. The presence of hIGFBP2 in the absence of exogenous IGF1 (not ruling out the possibility of endogenous- or cell-derived IGF1 in the media) activated IGF1R, which only occurred in the presence of MDA-9/Syntenin (Fig. 5A; Supplementary Fig. S6A). Enhanced STAT3 activation was also observed in these samples. These findings support the importance of MDA-9/Syntenin in IGF1R–mediated STAT3 activation. Further experiments revealed that MDA-9/Syntenin physically interacts and colocalizes with IGF1R (Fig. 5B and C), which might play an essential role in transmitting activation signals to STAT3. To obtain more insight into potential binding site(s) and the consequences of this interaction, we overexpressed different deletion mutants (ΔPDZ1 and ΔPDZ2) of *mda-9/syntenin* in RWPE-1 cells and examined IGF1R activation (Fig. 5D; Supplementary Fig. S6B). Expression of a PDZ1-deleted fragment (ΔPDZ1) failed to activate IGF1R (following hIGFBP2 treatment), indicating that the potential binding site of IGF1R resides in the PDZ1 domain of MDA-9/Syntenin. STAT3 activity also correlated with IGF1R activation, further confirming that MDA-9/Syntenin-mediated STAT3 activation is a downstream consequence of MDA-9/IGF1R interactions. Two prostate cancer cells, with genetically modified *mda-9/syntenin* expression (using Ad.5/3-sh*mda-9*), were exposed to exogenous hIGFBP2 to investigate IGF1R activation. As anticipated, lack of *mda-9/syntenin* expression robustly affected IGFBP2 activity (Fig. 5E; Supplementary Fig. S6C).

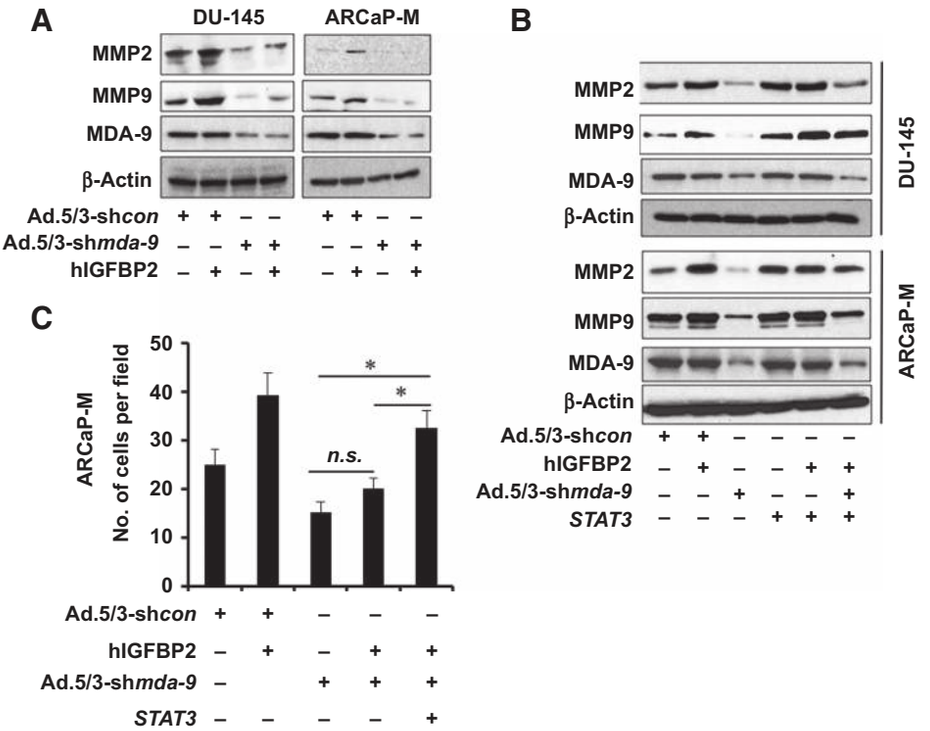

Figure 6.
MMP2 and MMP9 are key regulators of MDA-9/Syntenin-mediated prostate cancer invasion. **A,** Prostate cancer cell lines were infected with Ad.5/3-sh*con* or Ad.5/3-sh*mda-9* for 48 hours at 100 pfu/cell. Cells were reseeded on fibronectin-coated plates and were treated with recombinant hIGFBP2 (100 ng/mL) for 1 hour. Western blotting was done to determine MMP2 and MMP9 expression. **B,** Cells were cotransfected/infected with different adenovirus/plasmids, followed by 48-hour incubation for transgene expression. Western blotting was performed using anti–MMP2 and anti–MMP9. **C,** Cells were cotransfected with different expression plasmids. Forty-eight hours later, cells were trypsinized and invasion determined. Average with SD from three independent experiments. *, statistical significance ($P < 0.05$) between indicated groups.

Based on prior studies with MDA-9/Syntenin (11, 15, 16) and current experimental evidences, we hypothesized that MDA-9/Syntenin and IGF1R physically interact, enhancing stability and activating STAT3 through phosphorylation at tyrosine 705. Phospho-STAT3 forms a dimer and translocates into the nucleus to induce various genes that actively participate in prostate cancer progression. To test this hypothesis, we determined the expression of MMP2 and MMP9, the most common, invasion-related downstream targets of STAT3 in *mda-9/syntenin*-knockdown cell variants (transient or stable). Knocking down *mda-9/syntenin* downregulated basal expression of MMP2 and MMP9 (Fig. 6A; Supplementary Fig. S7A and S7B). Exogenous stimulation (using recombinant hIGFBP2) upregulated both proteins in wild-type cells; however, this did not occur in *mda-9/syntenin*–downregulated cells. These data and that provided in Fig. 4F (hIGFBP2–mediated STAT3 activation) demonstrate that endogenous MDA-9/Syntenin expression is critical for IGFBP2-mediated MMP2 and MMP9 upregulation through STAT3 activation. *mda-9/syntenin*-mediated downregulation of MMP2 and MMP9 was rescued when overexpressing a constitutively active STAT3 (Fig. 6B and C; Supplementary Fig. S8A and S8B). To confirm these findings, we developed two stable *mda-9/syntenin* knockout variant ARCaP-M cells using the CRISPR/Cas9 approach, one with minimal (Pool 1) and the other with a complete knockout (Pool-2; Fig. 7A) of expression. These knockout pools showed a significant downregulation of *igfbp2* (Fig. 7B), *MMP2* (Fig. 7C), and *MMP9* (Fig. 7C) mRNA. In addition, qPCR data from the complete knockout MDA-9/Syntenin cells (Pool 2) demonstrated a significant downregulation of STAT3 downstream targets, e.g., *IL6*, *IL8*, and *VEGFA* mRNA, further supporting the critical role of MDA-9/Syntenin in regulating STAT3 activity in prostate cancer (Fig. 7D). These clones significantly lose their invasive potential *in vitro* in Boyden chamber assays, and this phenotype is rescued significantly by a constitutive active STAT3 (Fig. 7E). A hypothetical model for MDA-9/Syntenin in regulating prostate cancer progression via IGF1R/STAT3 regulation is shown in Fig. 7F.

Discussion

Using computational-based analyses to interrogate online public data bases, confirmation was provided for the potential clinical significance of *mda-9/syntenin* with cancer prognosis (8). The bioinformatics data established and supported previous preclinical observations, indicating a correlation of MDA-9/Syntenin with glioblastoma (GBM; ref. 13) and melanoma (11) pathogenesis in clinical settings. Scrutiny of the public databases also predicted a relationship between MDA-9/Syntenin expression and prostate cancer prognosis. Moreover, it has been suggested that MDA-9/Syntenin is present in secreted exosomes (36), where its function requires clarification. Our present study confirms a direct relationship between expression of *mda-9/syntenin* and prostate cancer progression and provides direct molecular mechanistic insights into precisely how this gene regulates prostate cancer invasion (Fig. 7).

MDA-9/Syntenin is an adaptor scaffold protein that elicits its diverse functions by physically interacting with subsets of unique proteins in different regions of the cell (7, 9). In melanoma, MDA-9/Syntenin physically interacts with Src (16) activating the transcription factor NFκB, resulting in upregulation of invasion/angiogenesis-associated genes (e.g., MMP9, IGFBP2). EGFR and MDA-9/Syntenin interaction was observed in urothelial cancer (12) and in radiotherapy-treated GBM (37)

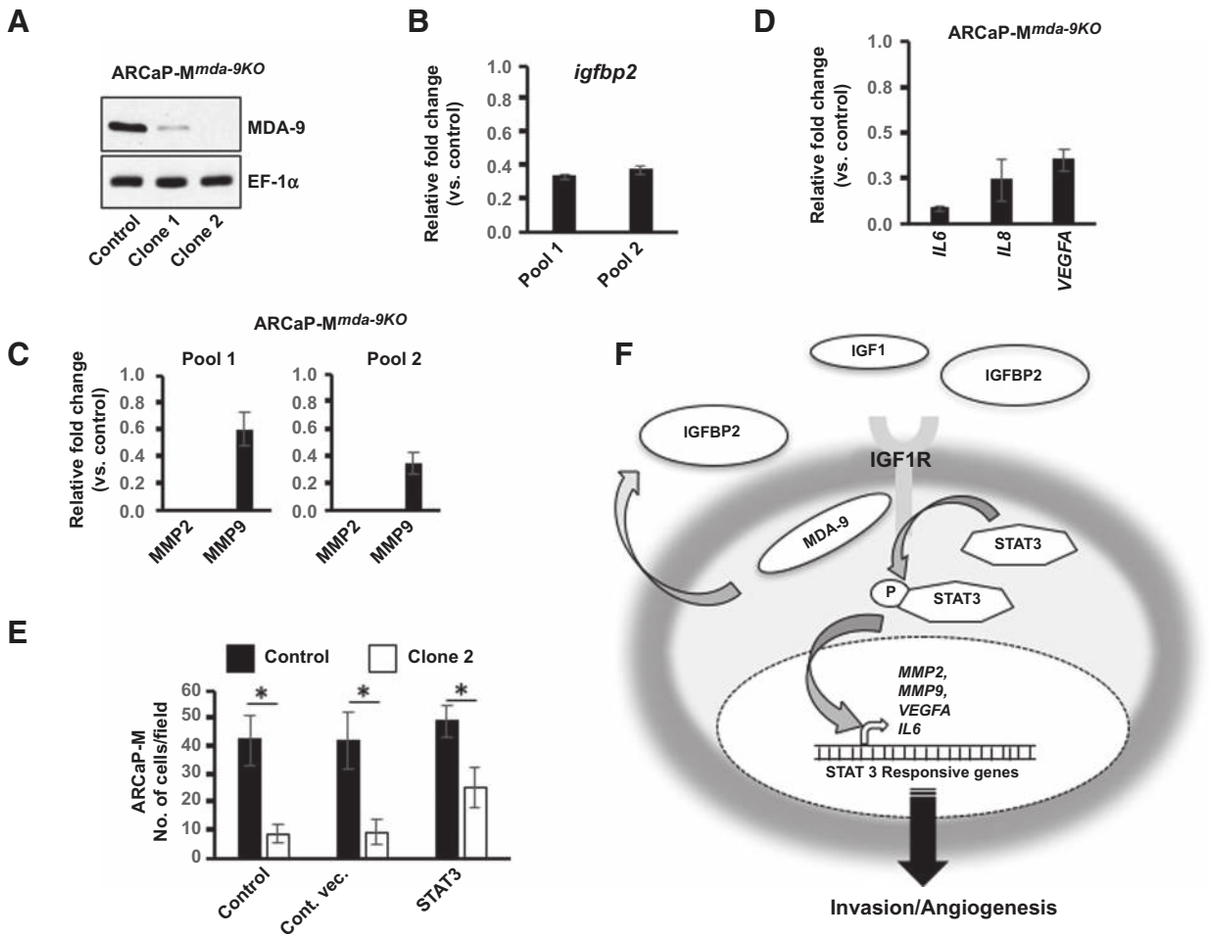

Figure 7.

Knockout of MDA-9/Syntenin in prostate cancer inhibits invasion. **A,** MDA-9/Syntenin expression in two clones from CRISPR/Cas9-*mda-9/syntenin*-transfected cells. **B** and **C,** Expression of *igfbp2* (**B**) or *MMP2* and *MMP9* mRNA (**C**), determined in Pool-1 and Pool-2, presented as fold-change vs. control CRISPR/Cas9-transfected cells. **D,** Expression of indicated mRNA determined in Pool-2. Data presented as fold change vs. control. **E,** Cells cotransfected with different expression plasmids. Forty-eight hours later, cells were trypsinized and invasion was determined. Cells were counted using brightfield microscopy. Average with SD from three independent experiments. *, statistical significance ($P < 0.05$) between indicated groups. **F,** Hypothetical model of MDA-9/Syntenin-mediated prostate cancer progression.

cells. Menezes and colleagues demonstrated a physical interaction of MDA-9/Syntenin with TGFβ that induced EMT in breast cancer cells (29). Interestingly, MDA-9/Syntenin was also reported as a partner of the cytoplasmic domain of TGFβ receptor in the context of breast cancer (38). In head and neck cancer, small proline-rich protein 1B interacts with the PDZ domain of MDA-9/Syntenin, regulating angiogenesis by upregulating VEGF-R (39). In addition, a number of interacting partners and the consequences of these interactions have been documented in noncancerous conditions. MDA-9/Syntenin interacts with the cytoplasmic domain of CD4 in T-helper cells allowing successful HIV entry (40). MDA-9/Syntenin and ALIX interactions are essential for exosome biogenesis (41). T-cell migration toward a chemoattractant is regulated by an association of MDA-9/Syntenin and myosin phosphatase Rho interacting protein (42). Thus, the diversity of interactions and the corresponding signaling changes in different cancerous or noncancerous disorders suggests that specific interactions might be context dependent and influenced by both intrinsic (e.g., affinity, availability) and extrinsic (ECM, growth factors) factors. Defining the precise role of MDA-9/Syntenin in diverse pathologic conditions is of value in clarifying its complete repertoire of functions. Our present study identified IGF1R as a new MDA-9/Syntenin binding partner. Ligensa and colleagues identified a type I PDZ domain binding site ((S/T)XV) at the C-terminal of IGF1R that could serve as the docking site for MDA-9/Syntenin (43). Further studies are necessary to define the critical genetic site(s) involved in defining IGF1R-MDA-9/Syntenin interactions and what additional partner proteins may facilitate or antagonize these interactions.

Following IGF1R binding to MDA-9/Syntenin, STAT3 is activated. STAT3 is one of the downstream targets of IGF1R. For example, Zong and colleagues demonstrated activation of STAT3 by phosphorylation at tyrosine 705 position by IGF1R upon IGF1 stimulation (35). In pancreatic cancer, an IGF1R–targeted small-molecule inhibitor NVP-AEW541 elicited a direct effect on cell

proliferation and abrogated cellular migration through inhibition of STAT3 activation (44). NT157, another IGF1R–targeting molecule, similarly caused significant downregulation of IGF1R in a preclinical model of metastatic melanoma progression (45). A role of IGF1R–mediated STAT3 activation (31) also occurs in prostate cancer, and its clinical relevance has been described (32). In summary, these studies and our previous collaborative study demonstrating that IL6 activates STAT3 through IGF1R in prostate cancer (31) establish a link between IGF1R and STAT3 activation. These observations raise intriguing questions as to how STAT3 is recruited by IGF1R. One study demonstrated that RACK1, an adaptor protein, served as a mediator and facilitated the recruitment of STAT3 with IGF1R for phosphorylation (46). Theoretically, being an adaptor protein, MDA-9/Syntenin may enable the assembly of a large complex containing both STAT3 and IGF1R proteins, which requires experimental confirmation. Apart from inflammation, active STAT3 transcriptionally regulates various genes involved in survival, proliferation, invasion, and angiogenesis (47). Because MDA-9/Syntenin did not show any direct impact on cell survival or proliferation in prostate cancer cells based on *in vitro* experiments, we predict that MDA-9/Syntenin-mediated upregulation of STAT3 activity may be more relevant in regulating cell invasion rather than cell survival, which is experimentally supported in our present study.

Expression of IGFBP2 is upregulated in prostate cancer patients. Recently, a meta-analysis using 17 prospective and two cross-sectional data, which included more than 10,000 patients and healthy volunteers, demonstrated a positive correlation of IGFBP2 with prostate cancer risk. Along with IGFBP2, this study also revealed that levels of IGF1, IGF2, and IGFBP-3 positively correlated with disease progression (48). IGFBP2 modulates IGF1 function through IGF1R. However, IGFBP2 may also function in an IGF1–independent manner via association with cytoplasmic or nuclear binding partners. Using cell fractionation approaches, IGFBP2 was shown to translocate into the nucleus through importin-α, via a classical nuclear import mechanism, and activated VEGFA transcription in multiple types of cancer including prostate cancer (49). IGFBP2 mediates EGFR-dependent STAT3 activation in glioblastoma cells. Although the activation of IGF1R was not explored, IGFBP2 and EGFR colocalized and accumulated in the nucleus, transactivated STAT3, and initiated the transcription of several STAT3-regulated genes including *c-Myc*, *Bcl-xL*, and *cyclin D* (50). Our experimental evidences suggest a potential role of IGFBP2 in activation of STAT3 through IGF1R in prostate cancer, where MDA-9/Syntenin plays a decisive role.

Support is now provided for a signaling cascade in which MDA-9/Syntenin physically interacts with IGF1R upon IGFBP2 stimulation, resulting in STAT3 phosphorylation, thereby facilitating the expression of invasion/angiogenesis-related genes particularly *MMP2*, *MMP9*, and *VEGFA* (Fig. 7). MDA-9/Syntenin-mediated MMP9 and VEGFA expression occurs in multiple cancers (11, 12). The present study firmly establishes MDA-9/Syntenin mechanistic functions in prostate cancer pathogenesis, principally through interactions with partner protein(s) that are influenced by IGFBP2, a protein upregulated and found in prostate cancer patients' body fluids (48). Although both PDZ domains are important for MDA-9/Syntenin function (16), recent studies confirm the importance of the PDZ1 domain in forming relevant interactions independent of the PDZ2 domain. As discussed, the PDZ1 domain of MDA-9/Syntenin is the interacting domain with TGFβ1 (29), TGFβ1 receptor (38), small proline-rich protein B (39), and now IGF1R. We demonstrate that disrupting the MDA-9/Syntenin/IGF1R/STAT3 loop profoundly affects prostate cancer pathogenesis, suggesting that targeting MDA-9/Syntenin could provide a strategy for inhibiting prostate cancer progression and metastasis. We recently developed a novel MDA-9/Syntenin PDZ1-targeted small-molecule pharmacologic agent (*PDZ1i*) using a combination of fragment-based drug discovery techniques guided by *in silico* docking and NMR-based design (37). This small molecule was efficacious in interrupting the interaction of MDA-9/Syntenin with EGFR and inhibited downstream signaling involved in the invasion gain in radiotherapy-surviving GBM cells. *PDZ1i* also displayed a strong synergistic effect when used in combination with radiotherapy in terms of survival in animals containing a primary human GBM (37). Further studies, not in the scope of this article, are clearly warranted to define the impact of *PDZ1i* on MDA-9/IGF1R interactions and downstream signaling events in prostate cancer progression and metastasis.

Disclosure of Potential Conflicts of Interest

P.B. Fisher has ownership interest (including patents) in Cancer Targeting Systems, Inc. and InVaMet Therapeutics, Inc., and is a consultant/advisory board member for InVaMet Therapeutics, Inc. No potential conflicts of interest were disclosed by the other authors.

Authors' Contributions

Conception and design: S.K. Das, P.B. Fisher
Development of methodology: S.K. Das
Acquisition of data (provided animals, acquired and managed patients, provided facilities, etc.): S.K. Das, A.K. Pradhan, P. Bhoopathi, S. Talukdar, X.-N. Shen, L. Emdad, P.B. Fisher
Analysis and interpretation of data (e.g., statistical analysis, biostatistics, computational analysis): S.K. Das, P.B. Fisher
Writing, review, and/or revision of the manuscript: S.K. Das, D. Sarkar, L. Emdad, P.B. Fisher
Study supervision: P.B. Fisher

Acknowledgments

The present research was supported in part by funding from NIH grant P50 CA058236 (to P.B. Fisher and Martin G. Pomper) and NCI Cancer Center Support Grant to VCU Massey Cancer Center P30 CA016059 (to P.B. Fisher and D. Sarkar), the National Foundation for Cancer Research (NFCR; to P.B. Fisher), the Human and Molecular Genetics Enhancement Fund (to S.K. Das and L. Emdad), VCU Massey Cancer Center (MCC) developmental funds (to P.B. Fisher), and VCU Institute of Molecular Medicine (VIMM) developmental funds (to P.B. Fisher, S.K. Das, and L. Emdad). Services and products in support of the research project were also provided by the VCU Massey Cancer Center Cancer Mouse Model Shared Resource, supported, in part, with funding from NIH-NCI Cancer Center Support Grant P30 CA016059 (to P.B. Fisher and D. Sarkar). P.B. Fisher holds the Thelma Newmeyer Corman Chair in Cancer Research in the MCC. D. Sarkar is the Harrison Foundation Distinguished Professor in Cancer Research in the MCC.

The costs of publication of this article were defrayed in part by the payment of page charges. This article must therefore be hereby marked *advertisement* in accordance with 18 U.S.C. Section 1734 solely to indicate this fact.

Received October 1, 2017; revised February 26, 2018; accepted March 19, 2018; published first March 23, 2018.

References

1. Sharifi N, Gulley JL, Dahut WL. Androgen deprivation therapy for prostate cancer. JAMA 2005;294:238–44.
2. Sarkar D, Fisher PB. Cancer metastasis: biologic basis and therapeutics. In: Welch DR, Lyden DC, Psaila C, editors. New York, NY: Cambridge University Press; 2011. p. 9.
3. Wan LL, Pantel K, Kang YB. Tumor metastasis: moving new biological insights into the clinic. Nat Med 2013;19:1450–64.
4. Jiang H, Fisher PB. Use of a sensitive and efficient subtraction hybridization protocol for the identification of genes differentially regulated during the induction of differentiation in human melanoma cells. Mol Cell Different 1993;1:285–99.
5. Lin JJ, Jiang HP, Fisher PB. Characterization of a novel melanoma differentiation-associated gene, mda-9, that is down-regulated during terminal cell differentiation. Mol Cell Differ 1996;4:317–33.
6. Lin JJ, Jiang H, Fisher PB. Melanoma differentiation associated gene-9, mda-9, is a human gamma interferon responsive gene. Gene 1998; 207:105–10.
7. Das SK, Bhutia SK, Kegelman TP, Peachy L, Oyesanya RA, Dasgupta S, et al. MDA-9/syntenin: a positive gatekeeper of melanoma metastasis. Front Biosci 2012;17:1–15.
8. Bacolod MD, Das SK, Sokhi UK, Bradley S, Fenstermacher DA, Pellecchia M, et al. Examination of epigenetic and other molecular factors associated with mda-9/syntenin dysregulation in cancer through integrated analyses of public genomic datasets. Adv Cancer Res 2015; 127:49–121.
9. Kegelman TP, Das SK, Emdad L, Hu B, Menezes ME, Bhoopathi P, et al. Targeting tumor invasion: the roles of MDA-9/Syntenin. Expert Opin Ther Targets 2015;19:97–112.
10. Koo TH, Lee JJ, Kim EM, Kim KW, Kim HD, Lee JH. Syntenin is overexpressed and promotes cell migration in metastatic human breast and gastric cancer cell lines. Oncogene 2002;21:4080–8.
11. Boukerche H, Su ZZ, Emdad L, Baril P, Balme B, Thomas L, et al. mda-9/Syntenin: a positive regulator of melanoma metastasis. Cancer Res 2005;65:10901–11.
12. Dasgupta S, Menezes ME, Das SK, Emdad L, Janjic A, Bhatia S, et al. Novel role of MDA-9/syntenin in regulating urothelial cell proliferation by modulating EGFR signaling. Clin Cancer Res 2013; 19:4621–33.
13. Kegelman TP, Das SK, Hu B, Bacolod MD, Fuller CE, Menezes ME, et al. MDA-9/syntenin is a key regulator of glioma pathogenesis. Neuro Oncol 2014;16:50–61.
14. Grootjans JJ, Zimmermann P, Reekmans G, Smets A, Degeest G, Durr J, et al. Syntenin, a PDZ protein that binds syndecan cytoplasmic domains. Proc Natl Acad Sci U S A 1997;94:13683–8.
15. Das SK, Bhutia SK, Azab B, Kegelman TP, Peachy L, Santhekadur PK, et al. MDA-9/syntenin and IGFBP-2 promote angiogenesis in human melanoma. Cancer Res 2013;73:844–54.
16. Boukerche H, Su ZZ, Prevot C, Sarkar D, Fisher PB. mda-9/Syntenin promotes metastasis in human melanoma cells by activating c-Src. Proc Natl Acad Sci U S A 2008;105:15914–9.
17. Das SK, Bhutia SK, Sokhi UK, Azab B, Su ZZ, Boukerche H, et al. Raf kinase inhibitor RKIP inhibits MDA-9/syntenin-mediated metastasis in melanoma. Cancer Res 2012;72:6217–26.
18. Khandwala HM, McCutcheon IE, Flyvbjerg A, Friend KE. The effects of insulin-like growth factors on tumorigenesis and neoplastic growth. Endocr Rev 2000;21:215–44.
19. Chan JM, Stampfer MJ, Giovannucci E, Gann PH, Ma J, Wilkinson P, et al. Plasma insulin-like growth factor-I and prostate cancer risk: a prospective study. Science 1998;279:563–6.
20. Kaplan-Lefko PJ, Sutherland BW, Evangelou AI, Hadsell DL, Barrios RJ, Foster BA, et al. Enforced epithelial expression of IGF-1 causes hyperplastic prostate growth while negative selection is requisite for spontaneous metastogenesis. Oncogene 2008;27:2868–76.
21. DiGiovanni J, Kiguchi K, Frijhoff A, Wilker E, Bol DK, Beltran L, et al. Deregulated expression of insulin-like growth factor 1 in prostate epithelium leads to neoplasia in transgenic mice. Proc Natl Acad Sci U S A 2000;97:3455–60.
22. Heidegger I, Massoner P, Sampson N, Klocker H. The insulin-like growth factor (IGF) axis as an anticancer target in prostate cancer. Cancer Lett 2015;367:113–21.
23. Playford MP, Bicknell D, Bodmer WF, Macaulay VM. Insulin-like growth factor 1 regulates the location, stability, and transcriptional activity of beta-catenin. Proc Natl Acad Sci U S A 2000;97: 12103–8.
24. Zhang D, Samani AA, Brodt P. The role of the IGF-I receptor in the regulation of matrix metalloproteinases, tumor invasion and metastasis. Horm Metab Res 2003;35:802–8.
25. Tao Y, Pinzi V, Bourhis J, Deutsch E. Mechanisms of disease: signaling of the insulin-like growth factor 1 receptor pathway–therapeutic perspectives in cancer. Nat Clin Pract Oncol 2007;4:591–602.
26. Dash R, Richards JE, Su ZZ, Bhutia SK, Azab B, Rahmani M, et al. Mechanism by which Mcl-1 regulates cancer-specific apoptosis triggered by mda-7/IL-24, an IL-10-related cytokine. Cancer Res 2010;70: 5034–45.
27. Ellwood-Yen K, Graeber TG, Wongvipat J, Iruela-Arispe ML, Zhang J, Matusik R, et al. Myc-driven murine prostate cancer shares molecular features with human prostate tumors. Cancer Cell 2003; 4:223–38.
28. Martin TA, Ye L, Sanders AJ, Lane J, Jiang WG. Cancer invasion and metastasis: molecular and cellular perspective. In:Jandial R, editor.Metastatic cancer: clinical and biological perspectives. Austin, TX: Landes Bioscience; 2013. p. 135–68.
29. Menezes ME, Shen XN, Das SK, Emdad L, Sarkar D, Fisher PB. MDA-9/Syntenin (SDCBP) modulates small GTPases RhoA and Cdc42 via transforming growth factor beta1 to enhance epithelial-mesenchymal transition in breast cancer. Oncotarget 2016;7:80175–89.
30. Xie TX, Wei D, Liu M, Gao AC, Ali-Osman F, Sawaya R, et al. Stat3 activation regulates the expression of matrix metalloproteinase-2 and tumor invasion and metastasis. Oncogene 2004;23:3550–60.
31. Rojas A, Liu G, Coleman I, Nelson PS, Zhang M, Dash R, et al. IL-6 promotes prostate tumorigenesis and progression through autocrine cross-activation of IGF-IR. Oncogene 2011;30:2345–55.
32. Tam L, McGlynn LM, Traynor P, Mukherjee R, Bartlett JM, Edwards J. Expression levels of the JAK/STAT pathway in the transition from hormone-sensitive to hormone-refractory prostate cancer. Br J Cancer 2007;97: 378–83.
33. Kimura G, Kasuya J, Giannini S, Honda Y, Mohan S, Kawachi M, et al. Insulin-like growth factor (IGF) system components in human prostatic cancer cell-lines: LNCaP, DU145, and PC-3 cells. Int J Urol 1996; 3:39–46.
34. Ho PJ, Baxter RC. Insulin-like growth factor-binding protein-2 in patients with prostate carcinoma and benign prostatic hyperplasia. Clin Endocrinol (Oxf) 1997;46:333–42.
35. Zong CS, Chan J, Levy DE, Horvath C, Sadowski HB, Wang LH. Mechanism of STAT3 activation by insulin-like growth factor I receptor. J Biol Chem 2000;275:15099–105.
36. Friand V, David G, Zimmermann P. Syntenin and syndecan in the biogenesis of exosomes. Biol Cell 2015;107:331–41.
37. Kegelman TP, Wu B, Das SK, Talukdar S, Beckta JM, Hu B, et al. Inhibition of radiation-induced glioblastoma invasion by genetic and pharmacological targeting of MDA-9/Syntenin. Proc Natl Acad Sci U S A 2017;114:370–5.
38. Hwangbo C, Tae N, Lee S, Kim O, Park OK, Kim J, et al. Syntenin regulates TGF-beta1-induced Smad activation and the epithelial-to-mesenchymal transition by inhibiting caveolin-mediated TGF-beta type I receptor internalization. Oncogene 2015;35:389–401.
39. Oyesanya RA, Bhatia S, Menezes ME, Dumur CI, Singh KP, Bae S, et al. MDA-9/Syntenin regulates differentiation and angiogenesis programs in head and neck squamous cell carcinoma. Oncoscience 2014;1:725–37.
40. Gordon-Alonso M, Rocha-Perugini V, Alvarez S, Moreno-Gonzalo O, Ursa A, Lopez-Martin S, et al. The PDZ-adaptor protein syntenin-1 regulates HIV-1 entry. Mol Biol Cell 2012;23:2253–63.
41. Baietti MF, Zhang Z, Mortier E, Melchior A, Degeest G, Geeraerts A, et al. Syndecan-syntenin-ALIX regulates the biogenesis of exosomes. Nat Cell Biol 2012;14:677–85.
42. Sala-Valdes M, Gordon-Alonso M, Tejera E, Ibanez A, Cabrero JR, Ursa A, et al. Association of syntenin-1 with M-RIP polarizes Rac-1 activation during chemotaxis and immune interactions. J Cell Sci 2012;125: 1235–46.

43. Ligensa T, Krauss S, Demuth D, Schumacher R, Camonis J, Jaques G, et al. A PDZ domain protein interacts with the C-terminal tail of the insulin-like growth factor-1 receptor but not with the insulin receptor. J Biol Chem 2001;276:33419–27.
44. Moser C, Schachtschneider P, Lang SA, Gaumann A, Mori A, Zimmermann J, et al. Inhibition of insulin-like growth factor-I receptor (IGF-IR) using NVP-AEW541, a small molecule kinase inhibitor, reduces orthotopic pancreatic cancer growth and angiogenesis. Eur J Cancer 2008;44:1577–86.
45. Flashner-Abramson E, Klein S, Mullin G, Shoshan E, Song R, Shir A, et al. Targeting melanoma with NT157 by blocking Stat3 and IGF1R signaling. Oncogene 2016;35:2675–80.
46. Zhang WZ, Zong CS, Hermanto U, Lopez-Bergami P, Ronai Z, Wang LH. RACK1 recruits STAT3 specifically to insulin and insulin-like growth factor 1 receptors for activation, which is important for regulating anchorage-independent growth. Mol Cell Biol 2006;26:413–24.
47. Jarnicki A, Putoczki T, Ernst M. Stat3: linking inflammation to epithelial cancer - more than a "gut" feeling? Cell Div 2010;5.
48. Travis RC, Appleby PN, Martin RM, Holly JMP, Albanes D, Black A, et al. A meta-analysis of individual participant data reveals an association between circulating levels of IGF-I and prostate cancer risk. Cancer Res 2016; 76:2288–300.
49. Azar WJ, Zivkovic S, Werther GA, Russo VC. IGFBP-2 nuclear translocation is mediated by a functional NLS sequence and is essential for its pro-tumorigenic actions in cancer cells. Oncogene 2014;33:578–88.
50. Chua CY, Liu Y, Granberg KJ, Hu L, Haapasalo H, Annala MJ, et al. IGFBP2 potentiates nuclear EGFR-STAT3 signaling. Oncogene 2016;35:738–47.